Supplementary Materials for

Long-Distance Integration of Nuclear ERK Signaling Triggered by Activation of a Few Dendritic Spines

Shenyu Zhai[1], Eugene D. Ark[1], Paula Parra-Bueno[3] and Ryohei Yasuda[1, 2, 3]*

*To whom correspondence should be addressed: Ryohei.Yasuda@mpfi.org

This PDF file includes:

Materials and Methods

Preparation

Organotypic hippocampal slice culture was prepared from postnatal day 6 or 7 rats, as previously described (*37*), in accordance with the animal care and use guidelines of Duke University Medical Center and Max Planck Florida Institute for Neuroscience. After 9-13 days in culture, CA1 pyramidal neurons were transfected with ballistic gene transfer (*38*) using gold beads (8–12 mg) coated with plasmids, and imaged 1-3 days after transfection.

2-photon fluorescence lifetime imaging

Details of fluorescence resonance energy transfer (FRET) imaging using a custom-built 2-photon fluorescence lifetime imaging microscope (2pFLIM) have been described previously (*39, 40*). $EKAR_{nuc}$ was simultaneously excited with a Ti:Sapphire laser (Maitai, Spectra-Physics) tuned at a wavelength of 920 nm. The fluorescence was collected by an objective (60x, 0.9 NA, Olympus), divided with a dichroic mirror (565 nm), and detected with two separated photoelectron multiplier tubes (PMTs) placed after wavelength filters (Chroma, HQ510/70-2p for green and HQ620/90-2p for red). For fluorescence lifetime imaging in the green channel, PMT with low transfer time spread (H7422-40p; Hamamatsu) was used. Fluorescence lifetime images were obtained using a time-correlated single photon counting board (SPC-150; Becker & Hickl) controlled with a custom software (*39, 41*).

2-photon glutamate uncaging

A second Ti:Sapphire laser tuned at a wavelength of 720 nm was used to uncage MNI-caged glutamate in extracellular solution with a train of 4-6 ms, 6-8 mW pulses (60 times at 1 Hz) at a spine of interest. Spine structural LTP (sLTP) was induced in Mg^{2+}-free artificial cerebrospinal fluid (ACSF; 130 mM NaCl, 2.5 mM KCl, 1.25 mM NaH_2PO_4, 25 mM $NaHCO_3$, 25 mM D-glucose, aerated with 95% O_2 and 5% CO_2) with 4 mM $CaCl_2$, 2 mM MNI-caged glutamate and 1 μM tetrodotoxin (TTX) (*3-5, 13*). The sustained volume change was calculated as the mean volume at 25-30 min for monomeric enhanced green fluorescent protein (mEGFP) neurons or 60-70 min for $EKAR_{nuc}$ neurons minus the mean baseline, normalized to the baseline volume. The transient volume change was calculated as the difference between the mean peak volume at ~ 1 min after uncaging and the sustained phase, normalized to the baseline volume (*13*).

2pFLIM data analyses

The mean fluorescence lifetime averaged over multiple populations τ_m was measured from the mean photon arrival time $\langle t \rangle$ as follows (*39*):

$$\tau_m = \langle t \rangle - t_0 = \frac{\int dt \cdot tF(t)}{\int dt \cdot F(t)} - t_0 \qquad \textbf{(Eq. S1)}$$

,

where $F(t)$ is the fluorescence decay curve after a short laser pulse, t is time, and t_0 is the time offset. We estimated the offset t_0 before each experiment by fitting fluorescence decay curve with double exponential function and comparing $\langle t \rangle$ with the fluorescence lifetime averaged over two populations as follows:

$$t_0 = \frac{\int dt \cdot tF(t)}{\int dt \cdot F(t)} - \tau_m \sim \frac{\int dt \cdot tF(t)}{\int dt \cdot F(t)} - \frac{P_1\tau_1^2 + P_2\tau_2^2}{P_1\tau_1 + P_2\tau_2}, \qquad \textbf{(Eq. S2)}$$

where P_1 and P_2 are the fraction and τ_1 and τ_2 are fluorescence lifetime of $EKAR_{nuc}$ in open and closed conformations obtained by fitting. Change in fluorescence lifetime is independent of t_0, thereby independent of model and curve fitting.

Basal τ_m and P_2 of $EKAR_{nuc}$ were 2.35 ± 0.04 ns and 21.6 ± 5% (mean ± SD), respectively. A small population of neurons (~25%) with high basal $EKAR_{nuc}$ FRET (τ_m < 2.29 or P_2 > 30 %) was discarded from further analyses because fluorescence lifetime did not change upon 7-spine stimulation in these neurons, perhaps due to the saturation of FRET signal.

<u>Ca^{2+} imaging</u>

For Ca^{2+} imaging with Fluo-4FF, we performed whole-cell patch clamping on CA1 pyramidal neurons using pipettes (4-5 MOhm) containing K^+-based internal solution under the current-clamp mode (*42*) (fig. S3). Included in the internal solution were a red Ca^{2+}-insensitive dye (300 μM Alexa 594) and a green Ca^{2+}-sensitive dye (500 μM Fluo-4FF). Recordings were made using a Multiclamp 700B amplifier, filtered at 10 kHz for current-clamp recordings, in Mg^{2+}-free ACSF plus 4 mM $CaCl_2$, 1 μM TTX and 2 μM MNI-caged glutamate. We acquired images every 64 ms while uncaging every 1024 ms. The $[Ca^{2+}]$ change ($\Delta[Ca^{2+}]$) was measured as:

$$\Delta[Ca^{2+}] \sim \frac{\left(\Delta G/R\right) \cdot K_D}{\left(G/R\right)_{max}}, \qquad \textbf{(Eq. S3)}$$

where $(G/R)_{max}$ is the ratio of green fluorescence intensity to red fluorescence intensity at saturating $[Ca^{2+}]$ (10 mM) measured in a pipette and K_D is 10 μM for Fluo-4FF (*16*). Simultaneously, uncaging-evoked excitatory postsynaptic potentials (uEPSPs) were recorded from the soma.

For Ca^{2+} imaging using GCaMP3, we transfected neurons with GCaMP3 (*43*) and imaged under a 2-photon microscope. We acquired images every 128 ms while uncaging every 1024 ms (fig. S4, A-G).

<u>Immunostaining</u>

Neurons in organotypic hippocampal slice culture were transfected with mEGFP using ballistic gene transfer (*38*). Slices having at least 2 transfected neurons were subjected to further analysis, and at least 1 transfected neuron in the slice was not stimulated and used as a negative control. Following 7-spine stimulation, the slices were incubated in imaging solution (Mg^{2+}-free ACSF) for further 45-90 min and fixed in 4% paraformaldehyde in phosphate buffered saline (PBS) at 4º C for >16 hours. The slices were then permeabilized and blocked at 4º C in PBS including 5% normal goat serum and 0.2% Triton-X100 (NGS/PBST). Immunostaining with primary antibodies was performed for 16 hours at 4º C using rabbit anti-phospho-CREB, anti-phospho-Elk-1, or anti-phospho-ERK antibodies (Cell Signaling) diluted in NGS/PBST. After 6 washes (5 min each) in NGS/PBST, the slices were incubated with a Texas-red or Alexa-568 conjugated secondary antibody (Invitrogen/Molecular Probes). All NGS/PBST contained

phosphatase inhibitors NaF (5 mM) and Na_3VO_4 (1 mM). To stain the nucleus, slices were incubated with 4',6-diamidino-2-phenylindole (DAPI; 1 μM) diluted in PBS for 5 min at room temperature. Images were acquired by a Leica SP5 laser scanning confocal microscope (Leica). Quantification of fluorescence intensity of phosphorylated proteins was performed by ImageJ (National Institute of Health).

Statistics

All data are presented as mean ± SEM, unless otherwise indicated. Asterisks denote statistical significance (*$P < 0.05$, **$P < 0.01$, ***$P < 0.001$). Statistical analysis was performed using one-way ANOVA followed by post-hoc test using the least significant difference.

Imaging nuclear ERK phosphorylation

To confirm that our 7-spine stimulation protocol activates ERK in the nucleus, we measured nuclear ERK activation by immunostaining for ERK phosphorylated at the sites essential for its activation (Thr202 and Tyr204 for ERK1 and Thr185 and Tyr187 for ERK2; fig. S1) (*44*). After glutamate uncaging at 7 spines of a CA1 neuron transfected with mEGFP, the slices were fixed and subjected to immunostaining with anti-phospho-ERK antibody. The level of ERK phosphorylation in the nucleus was quantified by measuring the immunofluorescence in the nuclei of the transfected neurons normalized to the average immunofluorescence in nuclei of 5 surrounding untransfected neurons. We found that the levels of phosphorylated ERK (pERK) in the uncaged neurons at 45 min and 75 min after 7-spine stimulation were higher than that in the unstimulated neurons (fig. S1, A and B). Thus, consistent with $EKAR_{nuc}$ imaging results (Fig. 1, F and G), our immunostaining data indicate that activation of 7 spines induced a slow and sustained increase in the level of pERK in the nucleus.

We also measured the level of pERK in the nucleus following 3-spine and 1-spine stimulation (fig. S1, C and D). Consistent with $EKAR_{nuc}$ imaging results (Fig. 2, A and B), pERK in the nucleus was unaltered following 1-spine stimulation, but significantly elevated following 3-spine stimulation. Finally, as a control for photodamage caused by uncaging laser, we measured the level of pERK in the nucleus 75 min after stimulation of 7 spines in the absence of caged glutamate (fig. S1E). As expected, there was no change in the level of pERK in the nucleus, suggesting that irradiation with laser alone does not induce nuclear ERK activation.

Imaging translocation of ERK2 into the nucleus

It has been suggested that translocation of active ERK2 into the nucleus is responsible for nuclear ERK activation during LTP (*8*). To test if nuclear translocation of ERK occurs in response to stimulation of a few spines, we performed live imaging of mEGFP-tagged ERK2 in organotypic slices. We co-transfected neurons with mEGFP-ERK2 and mRFP-mitogen activated protein kinase/ERK kinase (MEK)-1, and imaged mEGFP-ERK2. Co-expression of MEK1 is necessary for retaining overexpressed ERK2 in extra-nuclear region under basal condition due to the one-to-one stoichiometry of the mEGFP-ERK2 interaction with mRFP-MEK1 (*45-48*). Before stimulation, mEGFP-ERK2 was localized predominantly to the cytoplasm. Following 7-spine stimulation, mEGFP-ERK2 slowly accumulated in the nucleus and reached a plateau after ~60 min

(fig. S2). Following 1- and 3-spine stimulations, we observed no change and a significant increase in the level of mEGFP-ERK2 in the nucleus, respectively (fig. S2B and Fig. 2C). Thus, the relationship between the number of stimulated spines and mEGFP-ERK2 nuclear accumulation was similar to that between the number of stimulated spines and change in fluorescence lifetime of $EKAR_{nuc}$ (Fig. 2, A and B) or the level of pERK (fig. S1 and Fig. 2C). These results suggest that nuclear translocation of ERK2 is responsible, at least in part, for increased ERK activity in the nucleus following spine-specific activation.

Postsynaptic potential, Ca^{2+} elevation, and CaMKII activation in response to sLTP induction protocol

To examine the postsynaptic potentials and Ca^{2+} signals evoked by our sLTP induction protocol, we performed whole-cell patch clamp recordings using a patch pipette containing green Ca^{2+} indicator Fluo-4FF (K_d ~ 10 μM) together with Ca^{2+}–insensitive red fluorophore Alexa-594 (*42*). Ca^{2+} transients in spines were imaged under a 2-photon microscope and measured as changes in green fluorescence normalized to red fluorescence.

Under the current clamp mode, postsynaptic potentials during 60 uncaging pulses were 3.7 ± 1.3 mV for the 1st pulse and decayed to 1.6 ± 0.5 mV at the 60th pulse (mean ± SEM; fig. S3). The Ca^{2+} elevation in the stimulated spines showed a similar time course with a concentration of ~3.7 ± 1.3 μM at the 1st pulse and 0.6 ± 0.2 μM at the 60th pulse (n = 8 neurons). While Ca^{2+} significantly spread to the adjacent dendritic segment within ~1-2 μm, Ca^{2+} elevation at 4 μm from the stimulated spine was much smaller (6.3 ± 0.8% of Ca^{2+} transient in the stimulated spines; fig. S3). This result suggests that Ca^{2+} elevation is restricted to a few micrometers from the stimulated spines.

Since whole-cell dialysis inhibits sLTP (*13*) and potentially ERK activation in the nucleus, we also transfected neurons with GCaMP3, a genetically encoded Ca^{2+} indicator (*43*), and measured Ca^{2+} elevation in response to glutamate uncaging under a 2-photon microscope. In these experiments, we stimulated 7 spines to induce nuclear ERK activation (Fig. 1A) and simultaneously imaged fluorescence intensity change of GCaMP3 at the stimulated spines, nearby dendritic shafts, adjacent spines [located 2.1± 0.9 μm from the stimulated spines (mean ± SD; n = 41 spines)], and branch points in the primary dendrites [located 7.8 ± 3.3 μm from the stimulated spines (mean ± SD; n = 6 spines)]. The data indicated that Ca^{2+} elevation was highly compartmentalized in the stimulated spines with limited spreading into the dendritic shaft over 2-3 μm (fig. S4C), consistent with Fluo-4FF imaging (fig. S3) and previous studies (*3, 16*). From the post-hoc immunostaining experiment (similar to fig. S1), we confirmed that nuclear ERK activity increased in GCaMP3 neurons after stimulation (fig. S4E). The uncaging-induced Ca^{2+} elevation was dependent on NMDAR activation but not on either mGluRs or SERCA (fig. S4F). Qualitatively, signals indicated by GCaMP3 and fluo-4FF showed similar fluorescence changes upon uncaging (fig. S4G), except that the GCaMP3 signal showed much slower kinetics presumably due to its high Ca^{2+} affinity and slow off-rate (*43*). Overall, our Ca^{2+} imaging experiments (figs. S3 and S4) demonstrated that our stimulation protocol produces neither global Ca^{2+} elevation nor significant Ca^{2+} wave propagation.

To confirm that our sLTP protocol causes spine-specific plasticity, we measured calcium/calmodulin-dependent protein kinase II (CaMKII) activation in the stimulated and adjacent spines by performing 2pFLIM imaging of green-Camuiα, a FRET-based sensor for CaMKII (*4*) (fig. S4H). We observed strong activation of CaMKII in the stimulated spine. In contrast, in adjacent spines [located 2.7 ± 1.4 μm from the stimulated spines (mean ± SD; n = 57 spines)], neither CaMKII activation (fig. S4H) nor sLTP (fig. S4D) was induced, indicating that our stimulation triggers plasticity-inducing signal transduction only in the stimulated spines.

Calculation of diffusion coefficient of signal transmission

We observed a long delay (~ 40 min) in ERK activation in response to stimulation of distal dendrites (Fig. 2A). By assuming the signal emission from spines to the nucleus is caused by diffusion of molecules along dendrites, the diffusion coefficient (D) can be estimated from the one-dimensional diffusion equation:

$D \sim x^2 / (2t)$,

where $x \sim 200$ μm is the distance from the stimulated distal spines to the soma and $t \sim 40$ min is the onset. The obtained value, ~8 $\mu m^2/s$, is consistent with the reported diffusion coefficient of cytosolic ERK (*49*).

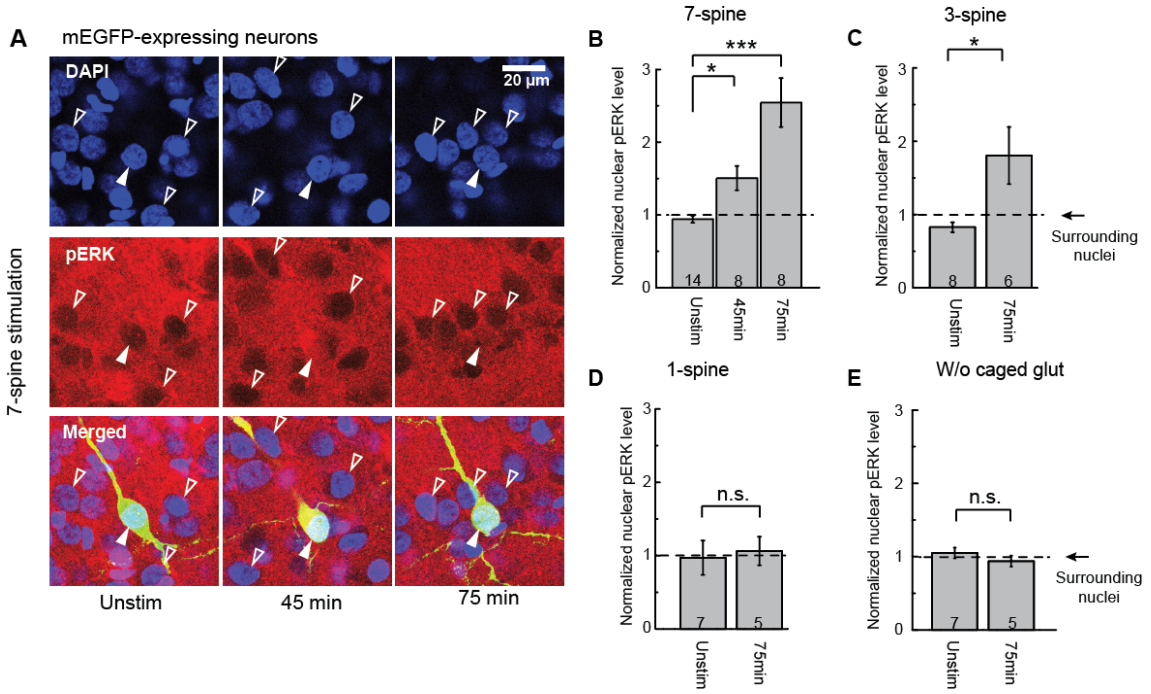

fig. S1

Stimulation of a few spines in a sequential fashion leads to increased nuclear phospho-ERK level as measured by immunostaining following stimulation of 7 spines. **(A)** Immunofluorescent images of phospho-ERK (pERK, red) in neurons expressing mEGFP (green, indicated by filled arrowheads) and surrounding untransfected neurons (examples indicated by open arrowheads). Shown are an unstimulated neuron ("Unstim"; left) and neurons fixed 45 min (middle) or 75 min (right) after stimulating 7 spines with 2-photon glutamate uncaging from the same slice. Nuclei were stained with DAPI (blue). The nuclear levels of pERK at 45 min and 75 min after 7-spine stimulation in the stimulated neurons were higher than that in the unstimulated neuron, suggesting activation of 7 spines induced a slow and sustained increase in ERK activity in the nucleus. Scale bar, 20 µm. **(B-E)** Quantification of the pERK immunofluorescence in the nuclei following 7-spine (B), 3-spine (C) and 1-spine (D) stimulation. As a control, we stimulated 7 spines in the absence of caged glutamate (E). The immunofluorescence in the nucleus (the location was identified with DAPI staining) of an mEGFP-expressing neuron was normalized to the averaged immunofluorescence in the nuclei of 5 surrounding untransfected neurons. Stimulated neurons were always paired with unstimulated neurons in the same slices (*15*). Quantification of sLTP of the same mEGFP-expressing neurons was shown in Fig. 1E. The numbers of neurons are indicated at the bottom the graphs. Data are means ± SEM. **P* < 0.05; ****P* < 0.001; n.s., not significant.

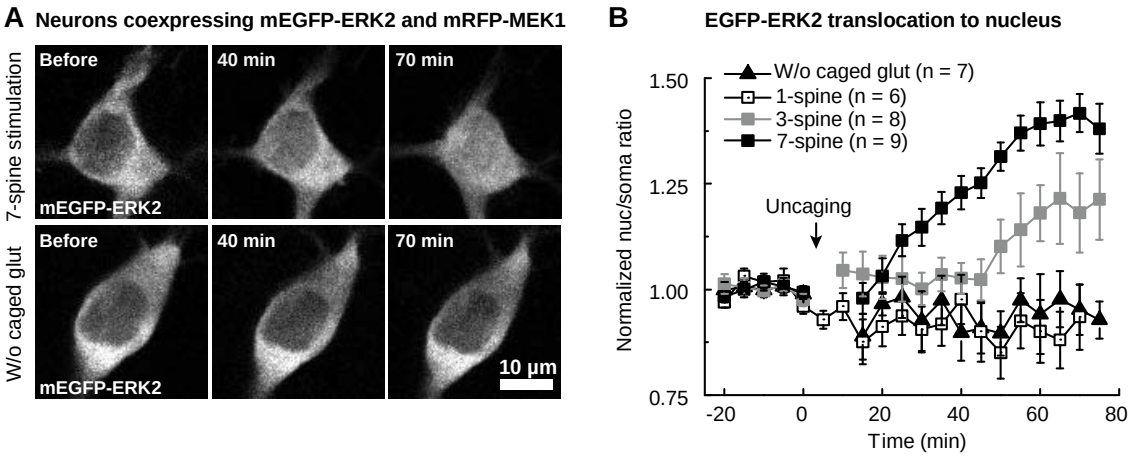

fig. S2

Glutamate uncaging at 7 spines induces nuclear translocation of ERK2. CA1 pyramidal neurons expressing mEGFP-ERK2 and mRFP-MEK1 were identified and stimulated by glutamate uncaging at 7 spines on proximal apical dendrites. Co-expression of mRFP-MEK1 is required to retain overexpressed mEGFP-ERK2 in the cytoplasm (*45-48*). **(A)** Two-photon imaging of mEGFP-ERK2 in hippocampal neurons with 7 spines stimulated with uncaging laser pulses in the presence ("7-spine stimulation") or absence of caged glutamate ("W/o caged glut"), respectively. Images of mEGFP-ERK2 distribution are shown for time points prior to uncaging (Before), at 40 and 70 min after uncaging (40 min, 70 min). Following 7-spine stimulation, mEGFP-ERK2 slowly accumulated in the nucleus. In the absence of caged glutamate, mEGFP-ERK2 remained predominantly cytoplastmic**. (B)** Time course of nuclear translocation of mEGFP-ERK2 in response to 1-, 3- and 7-spine stimulations in the presence of caged glutamate and 7-spine stimulation in the absence of caged glutamate (W/o caged glut). The fraction of mEGFP-ERK2 in the nucleus compared to that in the soma (i.e. nuclear/somatic ratio) was normalized to the baseline (-20 to 0 min).

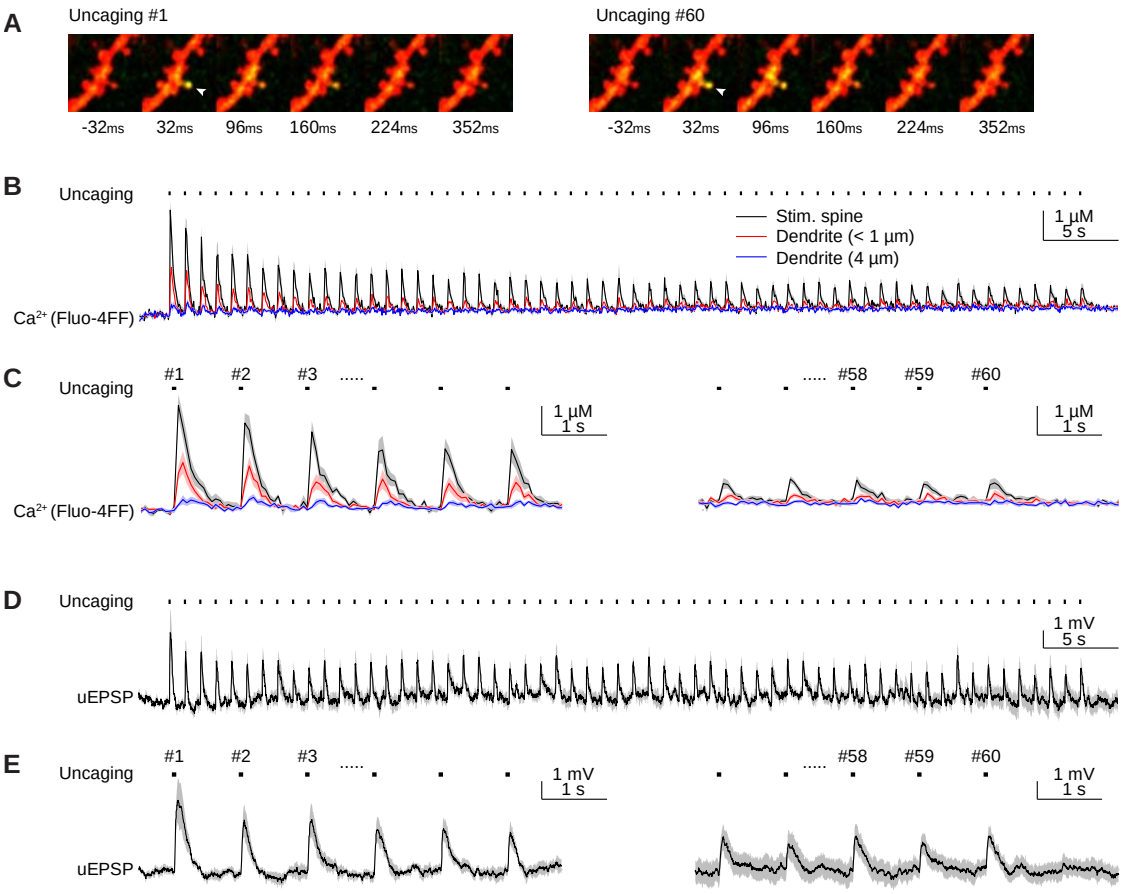

fig. S3

Postsynaptic potentials and Ca^{2+} elevation during sLTP protocol. **(A)** Dendritic spines of a CA1 pyramidal neuron loaded with Ca^{2+} indicator Fluo-4FF (green) and Alexa-594 (red) through a patch pipette. Uncaging laser pulses (5 ms) were applied near the spine indicated with a white arrowhead (60 pulses at 1024 ms intervals). **(B)** Ca^{2+} elevation in various locations during sLTP protocol measured with Fluo-4FF. Ca^{2+} elevation was restricted to the vicinity (< 4 µm) of the stimulated spines. We averaged 3-7 stimulated spines in each neuron (n = 8 neurons). **(C)** Close-up views of (B). **(D)** Uncaging-evoked excitatory postsynaptic potentials (uEPSPs) during sLTP protocol, in the same neuron as (B-C). **(E)** Close-up views of (D).

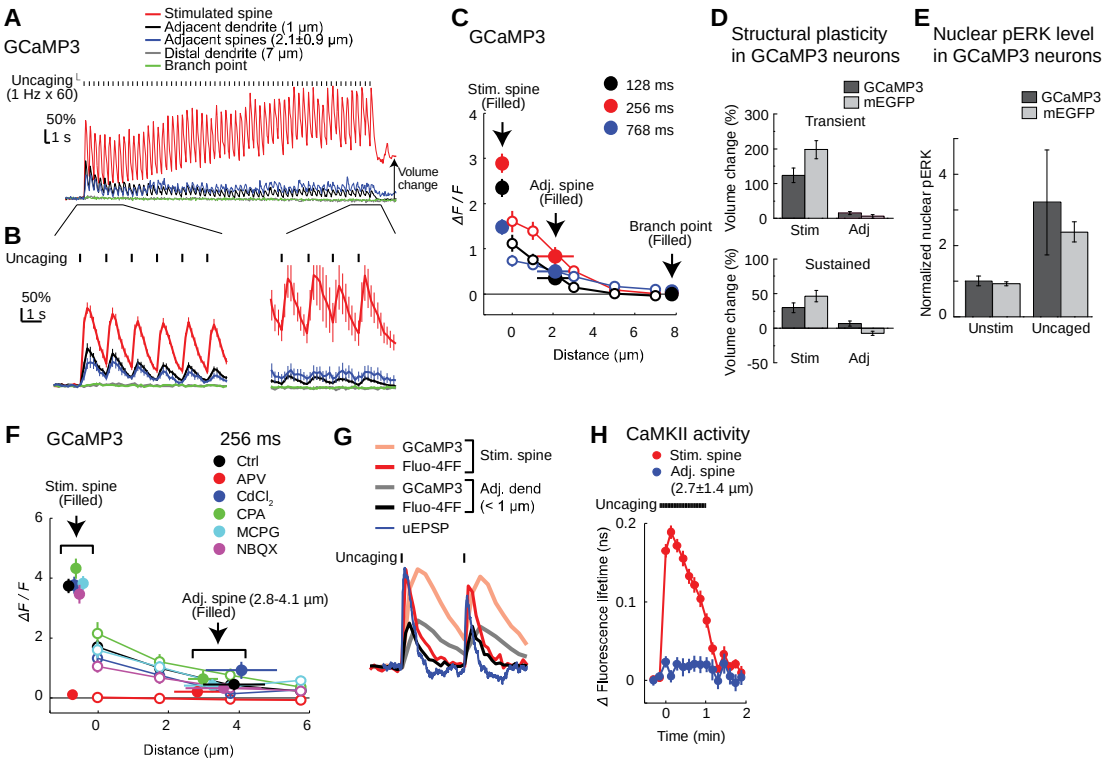

fig. S4

Ca^{2+} signaling during 7-spine stimulation measured with GCaMP3. **(A)** Fluorescence change of calcium indicator GCaMP3 at various locations during 7-spine stimulation which induces nuclear ERK activation [see (E)]. We averaged all 7 stimulated spines in each neuron (n = 6 neurons). Note that the slow fluorescence build-up in the baseline in the stimulated spine is due to spine enlargement. A single spine was stimulated with 5 ms uncaging pulses every 1024 ms (vertical bars on top), while imaged every 128 ms using 2-photon imaging. This protocol was repeated at 7 different spines with ~60 s intervals (Fig. 1A). **(B)** Close-up views of (A). **(C)** Quantification of spatial spreading of Ca^{2+} transient after the first uncaging pulse, at 128, 256, and 768 ms, respectively. Consistent with Fluo-4FF imaging, GCaMP3 fluorescence increase was restricted to the stimulated spine and nearby dendritic shaft (within 3-4 µm). **(D)** Quantification of spine volume change in the stimulated (Stim) and adjacent (Adj) spines in neurons expressing GCaMP3 or mEGFP in response to 7-spine uncaging. Note that GCaMP-expressing neurons still exhibited sLTP at the stimulated spines but not at adjacent spines. **(E)** In neurons expressing GCaMP3, the increase in nuclear pERK level induced by 7-spine stimulation was similar to that in neurons expressing mEGFP. GCaMP3: n = 3/3 (Unstim/Uncaged) neurons, the uncaged neurons were included in (A); mEGFP,: n = 14/8 (Unstim/Uncaged) neurons, same data as in fig. S1B. **(F)** Quantification of GCaMP3 signal triggered by uncaging in the absence (Ctrl, n = 48 spines) or presence of APV (50 µM, n = 32 spines), $CdCl_2$ (200 µM, n = 35 spines), CPA (20 µM, n = 26 spines), MCPG (1 mM, n = 35 spines) or NBQX (10 µM, n = 31 spines). **(G)** Comparison of the time courses of uncaging-evoked fluorescence signals obtained with GCaMP3 (A) and Fluo-4FF (fig. S3), as well as uEPSPs (fig. S3). **(H)** CaMKII activation in the stimulated and adjacent spines measured with green-Camuiα during uncaging. Note that CaMKII activation was highly restricted to the stimulated spines.

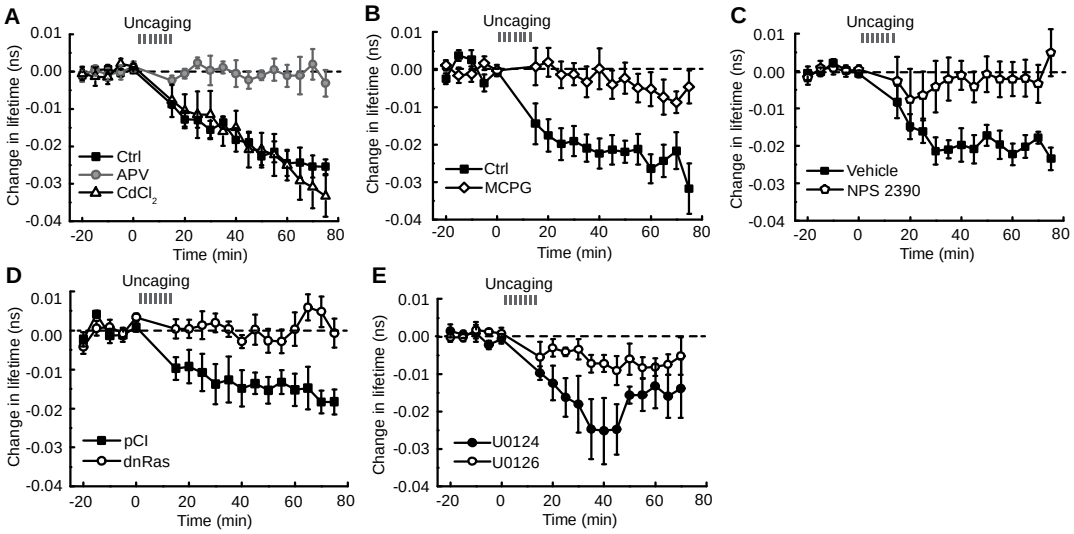

fig. S5

Nuclear ERK activation in response to 7-spine stimulation under manipulation of putative upstream signaling pathways. **(A** to **E)** Effects of pharmacological agents and genetic manipulation on the averaged time course of $EKAR_{nuc}$ fluorescence lifetime following 7-spine stimulation. For pharmacological experiments (A-C, E), slices were incubated with the indicated drugs for 30 min before experiments. The paired control experiments (black filled symbols) were performed with no vehicle in (A) and (B), 0.05% dimethyl sulfoxide (DMSO) as vehicle control in (C), or non-functional analog U0124 in (E). For (D), neurons were cotransfected with $EKAR_{nuc}$ together with dominant negative Ras (dnRas) or empty vector (pCI). The numbers of samples are 14 for Ctrl and 7 for APV and $CdCl_2$ in (A), 6 for Ctrl and MCPG in (B), 6 for Vehicle and NPS 2390 in (C), 7 for pCI and 8 for dnRas in (D), and 7 for U0124 and U0126 in (E). Data are means ± SEM.

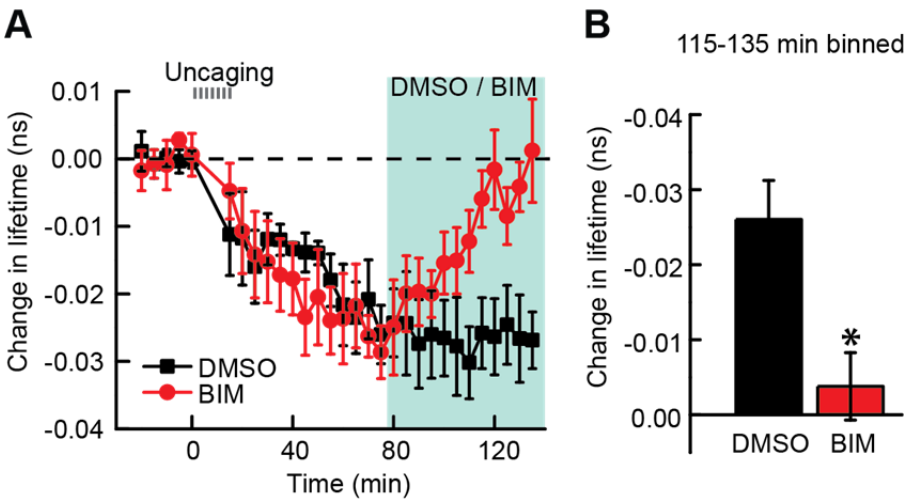

fig. S6

Sustained PKC activity is required for persistent nuclear ERK activation. **(A)** Time course of $EKAR_{nuc}$ fluorescence lifetime in response to 7-spine stimulation followed by delayed application of PKC inhibitor BIM or DMSO at 75 min (n = 5 neurons each). BIM gradually and completely reversed nuclear ERK activation induced by 7-spine stimulation. **(B)** Quantification of the effect of BIM on the persistence of nuclear ERK signaling as shown in (A) (averaged over 115-135 min; $*P < 0.05$).

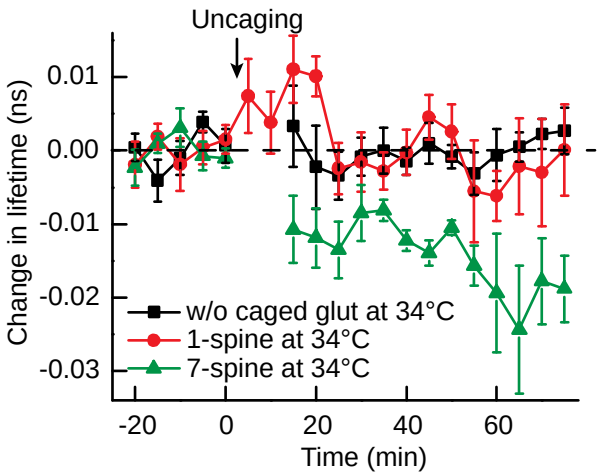

fig. S7
ERK is activated by 7-spine stimulation but not 1-spine stimulation at a near-physiological temperature (34°C). Data from control experiments in which 7-spine stimulation was performed in the absence of caged glutamate (w/o caged glut at 34 °C) are also shown (black).

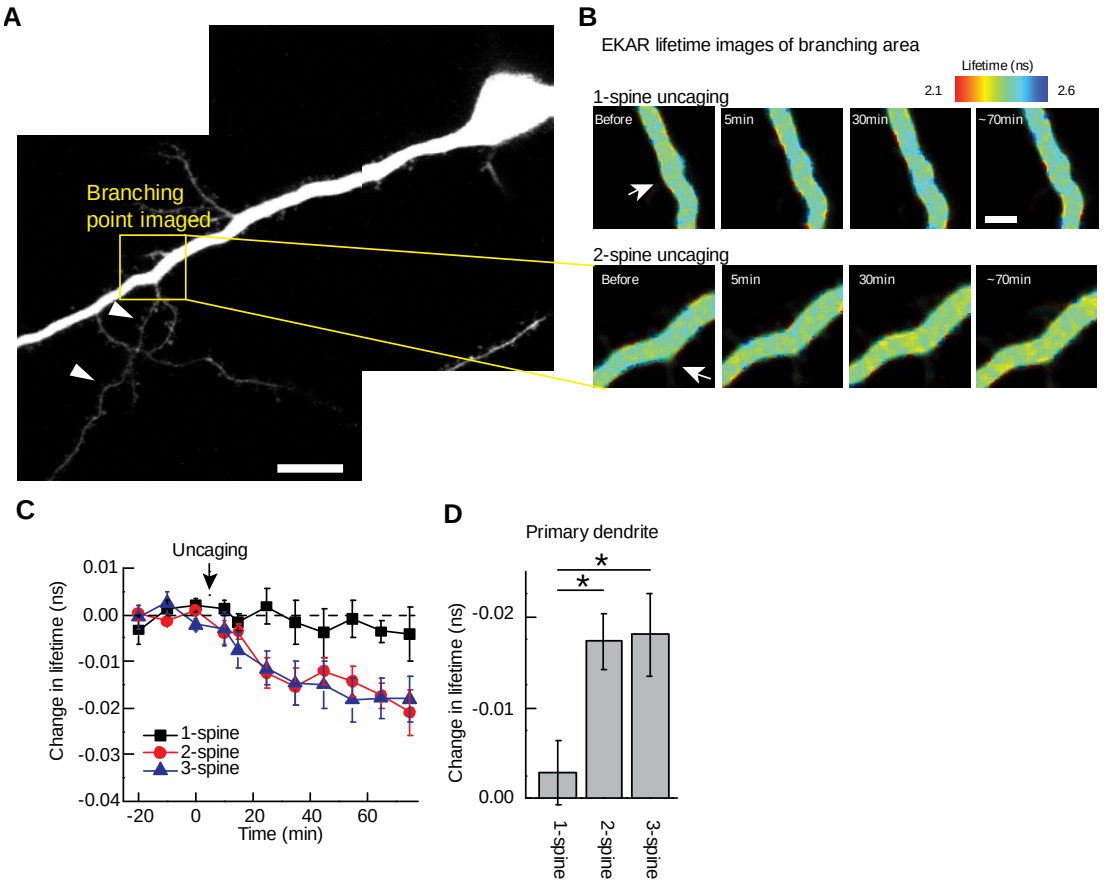

fig. S8

Activation of ERK in the branching area following glutamate uncaging. We expressed cytosolic EKAR ($EKAR_{cyto}$) together with $EKAR_{nuc}$ and imaged ERK activation at branching points in the primary dendrites in response to sequential stimulation of 1 to 3 spines in one branch with repetitive 2-photon glutamate uncaging. **(A)** A neuron transfected with $EKAR_{cyto}$ and $EKAR_{nuc}$. Two spines (white arrowheads) in a branch were stimulated with 2-photon glutamate uncaging (60 pulses, 1 Hz). Scale bar, 15 μm. **(B)** Fluorescence lifetime images at the branch point in response to 1-spine or 2-spine stimulation. The "2-spine uncaging" images were from the neuron shown in (A). Scale bar, 4 μm. ERK at the branching point in the primary dendrite was activated by 2-spine uncaging, as indicated by the appearance of warmer colors, but not by 1-spine uncaging. **(C)** Time course of EKAR fluorescence lifetime change at the branching point in response to 1-, 2-, or 3-spine stimulation in one dendritic branch (n = 5, 6 and 6 neurons, respectively). **(D)** Quantification of the plateau of fluorescence lifetime change in (C) (averaged over 40-70 min; $*P < 0.05$). Note that compared to 2-spine stimulation, 3-spine stimulation did not further increase ERK activity at the branching point in the primary dendrite.